

Mauna Kea turbulence statistics from the TMT MASS/DIMM and weather station at the 13 North site

Ralf Flicker, 2006-09-22

W.M. Keck Observatory, 65-1120 Mamalahoa Hwy., Kamuela, Hawaii 96743

ABSTRACT

This note summarizes the statistics of the TMT Mauna Kea MASS/DIMM data (TMT test site 13N) that has been gathered and analyzed so far. The current analysis includes measurements from June 2005 to August 2006. This analysis currently is ongoing and will be updated monthly as more data becomes available.

NOTE: As of the time of writing and until TMT has made the data public, certain information disclosed in this document, in particular that concerning overall statistics, must under no circumstances be distributed or communicated to the public.

NOTE 2: Most of the plots in this document were generated as EPSF files in IDL. Some of the embedded graphics (especially color fields) may not look correct on the computer display, but they will print correctly to a postscript printer.

1. Introduction

In an effort to better understand the atmospheric conditions on Mauna Kea as they affect astronomical observations, and in order to refine our turbulence models for upcoming NGAO (next-generation adaptive optics) modeling and design work, we have been given access to the most recent TMT site monitoring data for Mauna Kea. As part of their site selection and survey campaign, the TMT project has operated a turbulence and weather monitoring station on Mauna Kea since mid-2005, at the location designated as 13 North (13N), see Refs. [1] (Skidmore et al., 2004) and [2] (Riddle et al., 2006). The location of 13N is indicated in the lower right corner of image below. The turbulence measurement instruments include a differential image motion monitor (DIMM) that measures the seeing, and a multi-aperture scintillation sensor (MASS) that quantifies the free atmosphere seeing by in terms of a 6-layer vertical profile. Together these two instruments provide information that allows us to compute the statistical measures most commonly used in characterizing atmospheric turbulence in the context of astronomical adaptive optics (AO), i.e. the Fried parameter r_0 , the isoplanatic angle θ_0 , the laser guide star (LGS) focal anisoplanatism parameter d_0 (see Appendix A). In addition there is a weather station that records wind speeds and directions, temperature, relative humidity and atmospheric pressure at the altitude of the tower (some 20 ft above the ground).

Some initial efforts have also been made to correlate the 13N MASS/DIMM measurements to seeing measurements made at Keck (LGS AO checkout, NIRC2), but no conclusive results have yet been arrived at. This study is currently being undertaken in more detail and will be presented in a separate note. Also not included in the current text and to be investigated further is a study of the temporal statistics of turbulence parameters, such as e.g. correlation functions and temporal power spectra of r_0 and θ_0 .





2. Data analysis

The statistical results presented in this text were generated by an IDL script, and the next section (2.1) gives a brief instruction on how to run the code. Section 2.2 clarifies the selection criteria applied to the data, and discusses some potential selection effects that may bias the estimation of statistical turbulence parameters. The main results are presented in Sect. 2.3.

2.1. Analysis code

This section briefly outlines the code written to analyze the data, for anyone who wishes to rerun it and produce new statistics as more data becomes available, or to make modifications/enhancements to it. The code is written in IDL, and is currently only set up to be run on the Sun Java workstation “pakalana” (log in under the project account “kpaobl”). The routine “tmtmd.pro” resides in `/local/home/kpaobl/IDL/T6-Hawaii/` and this is also where the plots are saved by default. The script can be run by simply starting up IDL and typing “tmtmd” at the prompt. It takes the optional keywords “load” (to load analysis data from a previous session and go directly to the plotting sequence) and “win” (to set the postscript device to EPSF and include a Windows-friendly preview with the plots).

When the code is run (without the load keyword) it starts by reading in all the available MASS/DIMM data from Chris Neyman’s home directory on pakalana, `/local/home/cneyman/TMTarchive/results/` and in verbose mode (the default) it also prints out their corresponding file names as the files are imported and processed. The three types of files that are read are the DIMM summary, MASS profile and MASS summary files. For a full description of these file formats and their contents see Ref. [3] (Neyman 2006). The files are currently imported using the `read_ascii` function together with predefined ascii templates. So long as the format of these files do not change (i.e. the ordering of columns, rows, headers etc) additional MASS/DIMM data can simply be dumped into the same data directory and the code rerun to produce new statistics. If the formats of the files change (let’s hope this never happens), new templates will have to be created, and the code modified to handle multiple types of file formats accordingly.

2.2. Data selection

Currently the archive contains DIMM data from 2005-06-28 to 2006-08-31 and MASS data from 2005-07-28 to 2006-08-31. We were however advised to exclude all MASS data before December 2005, as the instrument during this time had been experiencing technical problems that rendered the data unreliable (M. Schöck, August 2006, private communication). Hence the MASS data presented here only covers 2005-12-01 to 2006-08-31. Aside from this, we have only discarded individual data entries from the MASS and DIMM data files where the measurement or the computation has obviously failed, as indicated by the non-physical values returned (NaN, Inf, negative or zero Strehl ratios reported by the DIMM, etc). These entries are possibly the result of an exposure being partly obscured by clouds, and/or by the numerical algorithm (which is performing an optimization and extrapolation of an ill-posed mathematical problem) failing to find a solution. Addressing potential selection effects that might bias the interpretation of the data, we include histograms of the two instruments’ duty cycles both hourly and monthly (cf. Figs. 2 and 7).

2.3. Results

Figures 1-5 and tables 1 and 2 present the results of the analysis carried out so far. For the mathematical definitions and formulas used in the computation of the various quantities presented, refer to Sect. 4. The computation of the ground layer turbulence coefficient c_0 according to Eqn. (14) required the combination of MASS and DIMM data. The DIMM r_0 was therefore interpolated to match the UTC time stamps of the MASS c_l coefficients, using a spline interpolation method. There is a tendency of the MASS computational algorithm to overshoot in strong scintillation and overestimate the turbulence strength. When this happens, the simple computation in (14) fails and returns a negative number. In Table 2 and Fig. 5, these occurrences have been excluded (3640 data entries out of 49914 total). It should be mentioned that the simple averaging of c_l coefficients over the year to produce an “average turbulence profile” is not a 100% representative presentation. A more careful investigation (to be undertaken in a future study) should attempt to identify the dominant two or three morphologies of the profile, and compute averages within each class. As an illustration of this point, the second and third layers (c_1 and c_2 , at 500 and 1000 m respectively) show a distinctly bifurcated distribution (cf. Fig. 5), in which they are either close to zero or the second and third strongest layers respectively. Thus computing the average will in most



cases misrepresent the actual shape of the profile. Also note that the sharp edges down at very low values in the “cloud plot” (left-hand graph) of Fig. 5 are believed to be numerical artifacts, and not a physical feature of the turbulence. This abnormality is currently under investigation.

Parameter		unit	Mean value	25% CDF	50% CDF	75% CDF
Seeing	θ	arc seconds	0.89	0.58	0.75	1.04
Fried parameter	r_0	cm	14.0	9.7	13.4	17.5
Isoplanatic angle	θ_0	arc seconds	2.79	1.87	2.58	3.44
Cone effect	d_0	m	5.09	3.37	4.69	6.32
Free atmosphere r_0	r^*	cm	36.2	17.1	30.1	47.6

Table 1. Overall mean, 25th, 50th and 75th percentiles (of cumulative density function, CDF) of the principal turbulence parameters extracted from the MASS/DIMM data. Refer to Sect. 4 for definitions of the parameters.

Altitude (m)	0	500	1000	2000	4000	8000	16000
<i>Average</i>							
c_l ($m^{1/3}$)	4.24e-13	4.64e-14	3.26e-14	2.70e-14	4.40e-14	3.06e-14	2.50e-14
c_l/μ_0	0.673	0.074	0.052	0.042	0.070	0.049	0.040
<i>35% central average</i>							
c_l ($m^{1/3}$)	4.03e-13	2.93e-14	3.74e-14	3.10e-14	4.73e-14	3.07e-14	2.69e-14
c_l/μ_0	0.666	0.048	0.062	0.051	0.078	0.051	0.044

Table 2. Average turbulence profiles at zenith, as represented by the integrated layer coefficients c_l and the fractional layer contribution c_l/μ_0 . Refer to Sect. 4 for definitions of the parameters. The second group called “35% central average” is the profile based on a 35% subset centered on the joint $\{r_0, \theta_0\}$ histogram (see Figs. 5 and 4).

3. References

1. W. Skidmore, M. Schöck, A. Tokovinin, G. Djorgovski, A. R. Walker, R. Blum, T. Travouillon, J. Seguel, E. Bustos, D. Walker, J. Vasquez, and P. E. Gillett, “The Thirty Meter Telescope site testing system,” Ground-based Telescopes, Edited by J. M. Oschmann Jr., Proceedings of the SPIE, **5489** (2004).
2. R. Riddle, M. Schöck, W. Skidmore, “The Thirty Meter Telescope site testing robotic computer system”, Space Telescopes and Instrumentation II: Ultraviolet to Gamma Ray. Edited by M. Turner; and G. Hasinger, Proceedings of the SPIE, **6267** (2006).
3. C. Neyman, “Accessing the Mauna Kea TMT seeing & weather data”, Keck note 2006-08-02, KPAOtech\SiteConditions\MaunaKeaSeeing\TMTmassdimNotes.doc
4. J. W. Hardy, “Adaptive Optics for Astronomical Telescopes,” Oxford University Press, Inc., New York (1998)

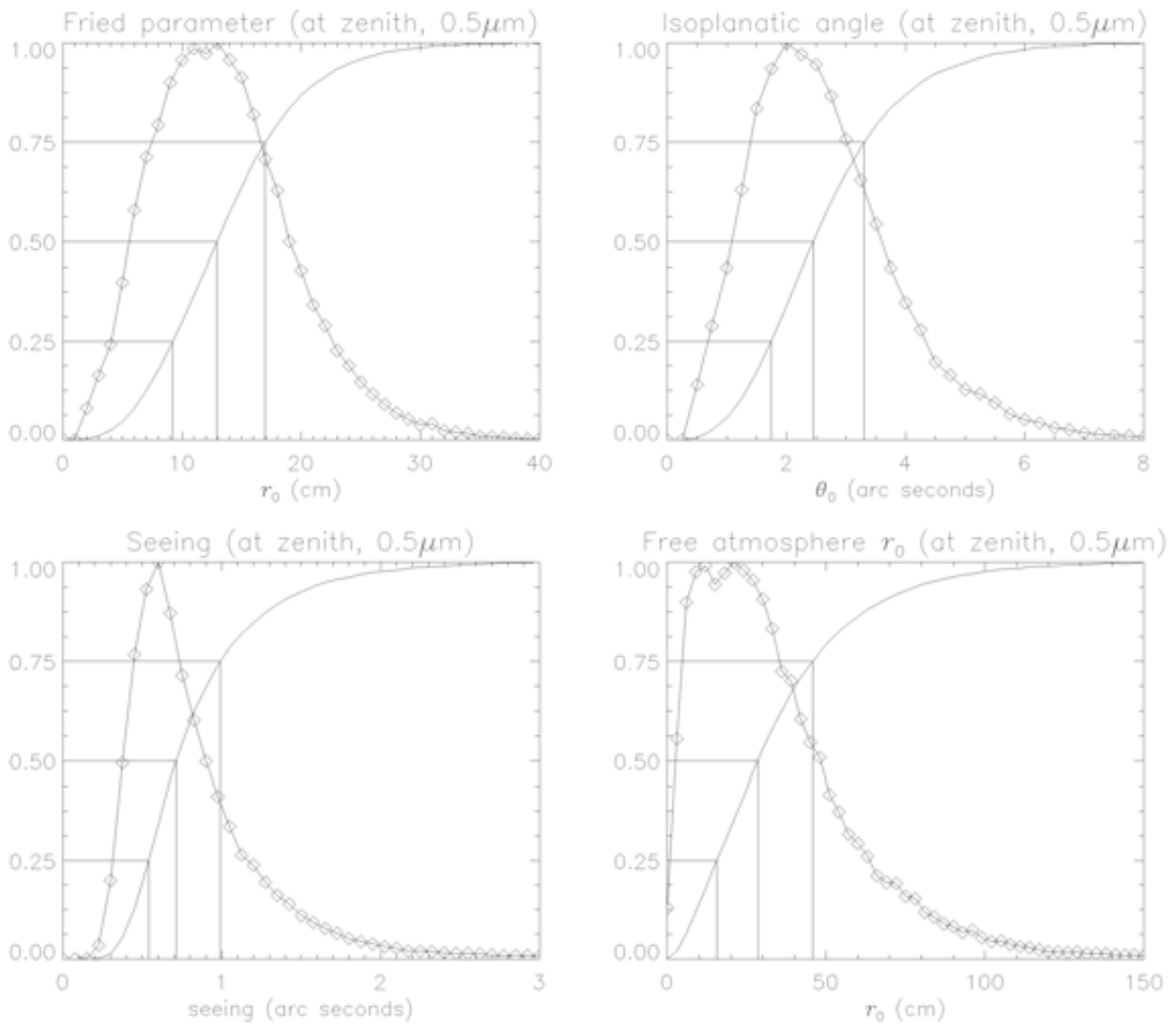


Fig. 1. Histograms (solid line plus diamond plot symbols) and cumulative density functions (CDFs) of the atmospheric parameters from Fig. 2. The y-axes are scaled to the CDFs, and the density functions have been scaled up (from unit integral) for display purposes. The three lines in each graph mark the 25th, 50th and 75th percentiles.

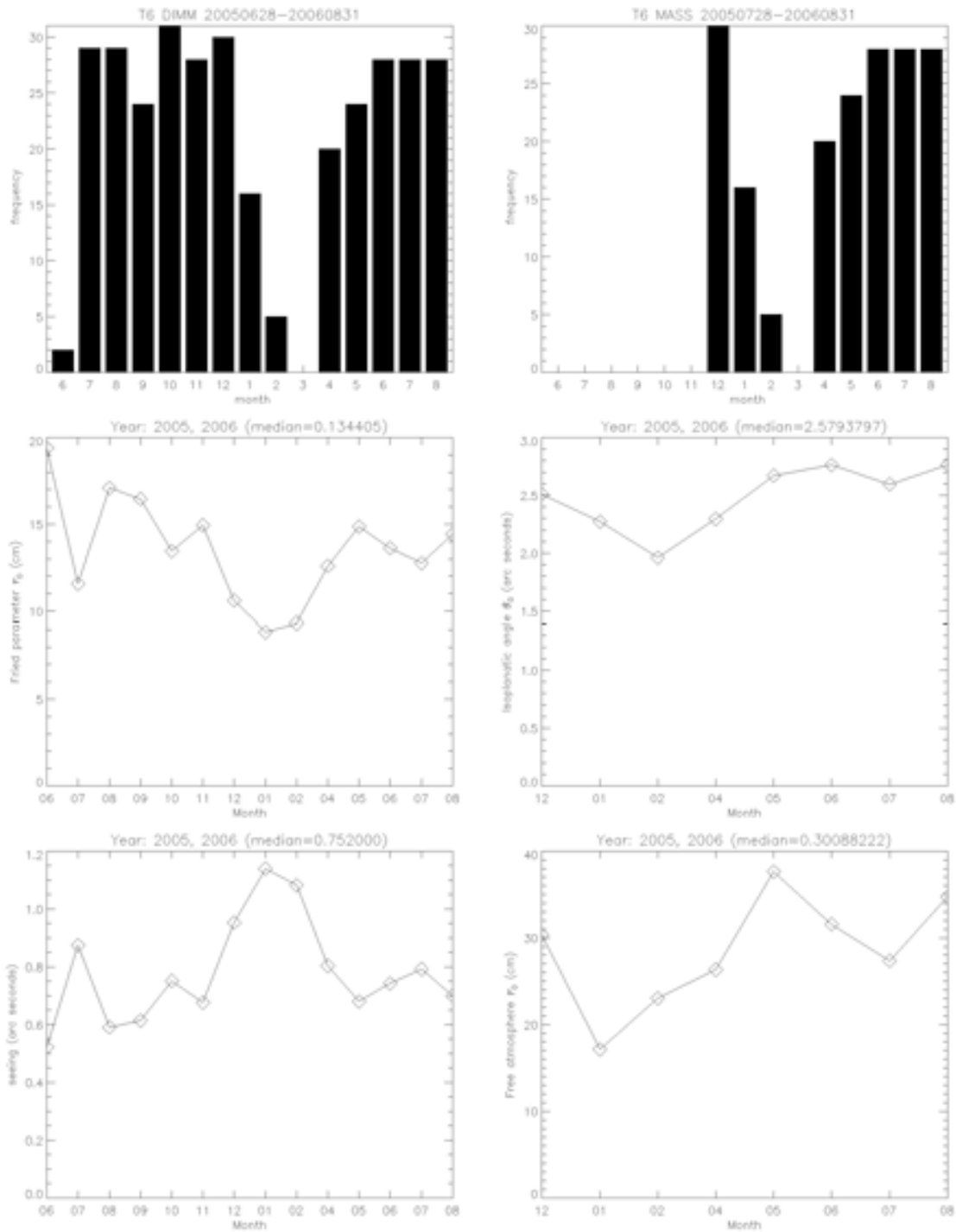


Fig. 2. Monthly variations of the median Fried parameter and seeing (DIMM – left column), and the median isoplanatic angle and free atmosphere r_0 (MASS – right column), with the overall medians quoted in the title of each figure. The top row shows the monthly duty cycle (days per month) for each instrument.

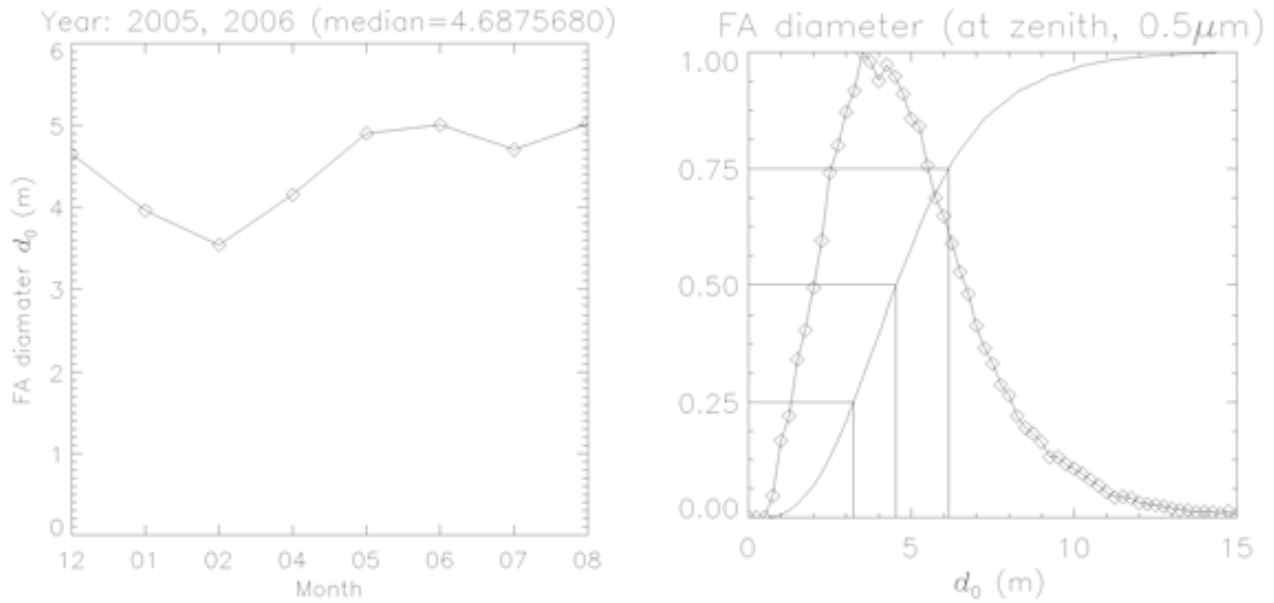


Fig. 3. The focal anisoplanatism (FA) parameter d_0 : monthly medians (left), and the overall histogram and cumulative density function (right). The overall median was 4.7 m, and the 25th, 50th and 75th percentiles are indicated on the abscissa in the right figure by the three lines.

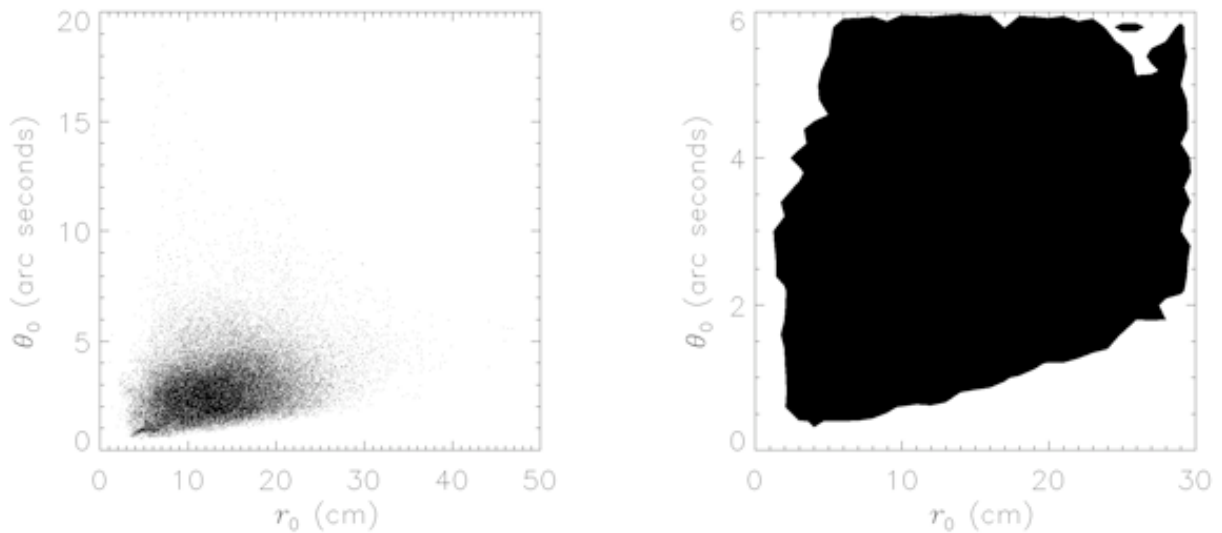


Fig. 4. Scatter plot and contour plot of the joint r_0 and θ_0 statistics.

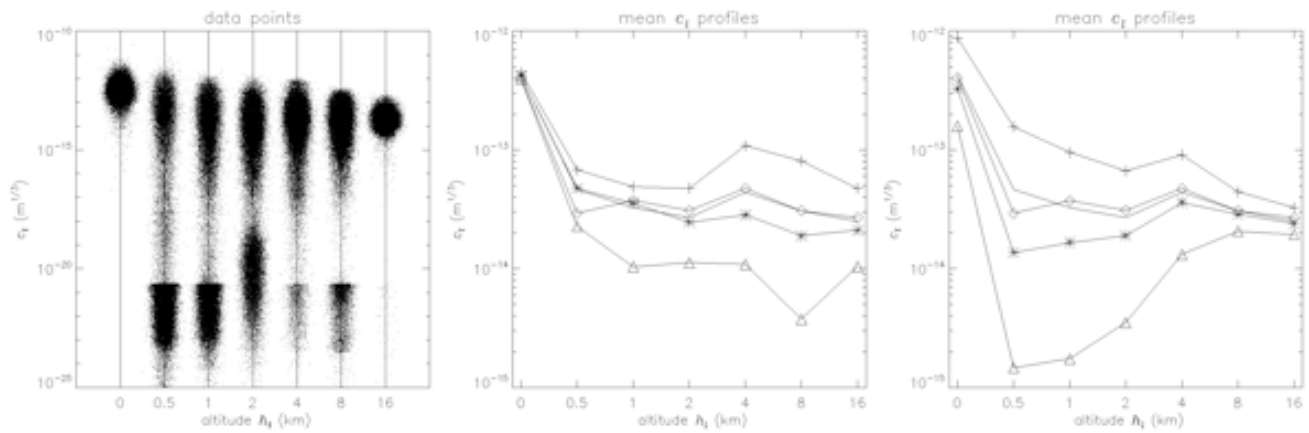


Fig. 5. Left: virtual density plot (or “cloud plot”) of the c_l coefficients as returned by the MASS. For visualization purposes, the data points corresponding to each altitude have been smeared out around the central x-value by a Gaussian distribution, in order to make the impression of density clearer to the eye. Middle and right: average turbulence profiles, in various sub-sets of r_0 and θ_0 statistics. The solid line without symbols is the average of each c_l over the entire data set. The asterisks are averages over the central 50% set, plusses and triangles are averages over the 25th and 75th percentiles, and diamonds are averages over a 35% set from the two-dimensional joint $\{r_0, \theta_0\}$ histogram (see Fig. 4).

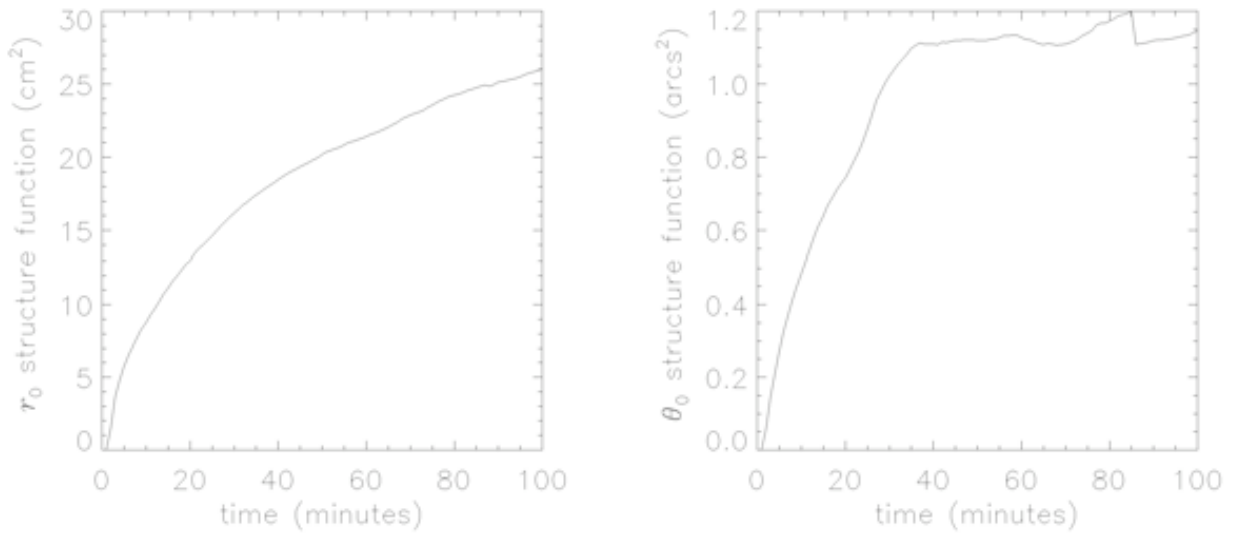


Fig. 6. Structure functions of r_0 and θ_0 . The θ_0 curve on the right is probably exhibiting some low number statistics as all data before December 2005 were discarded.

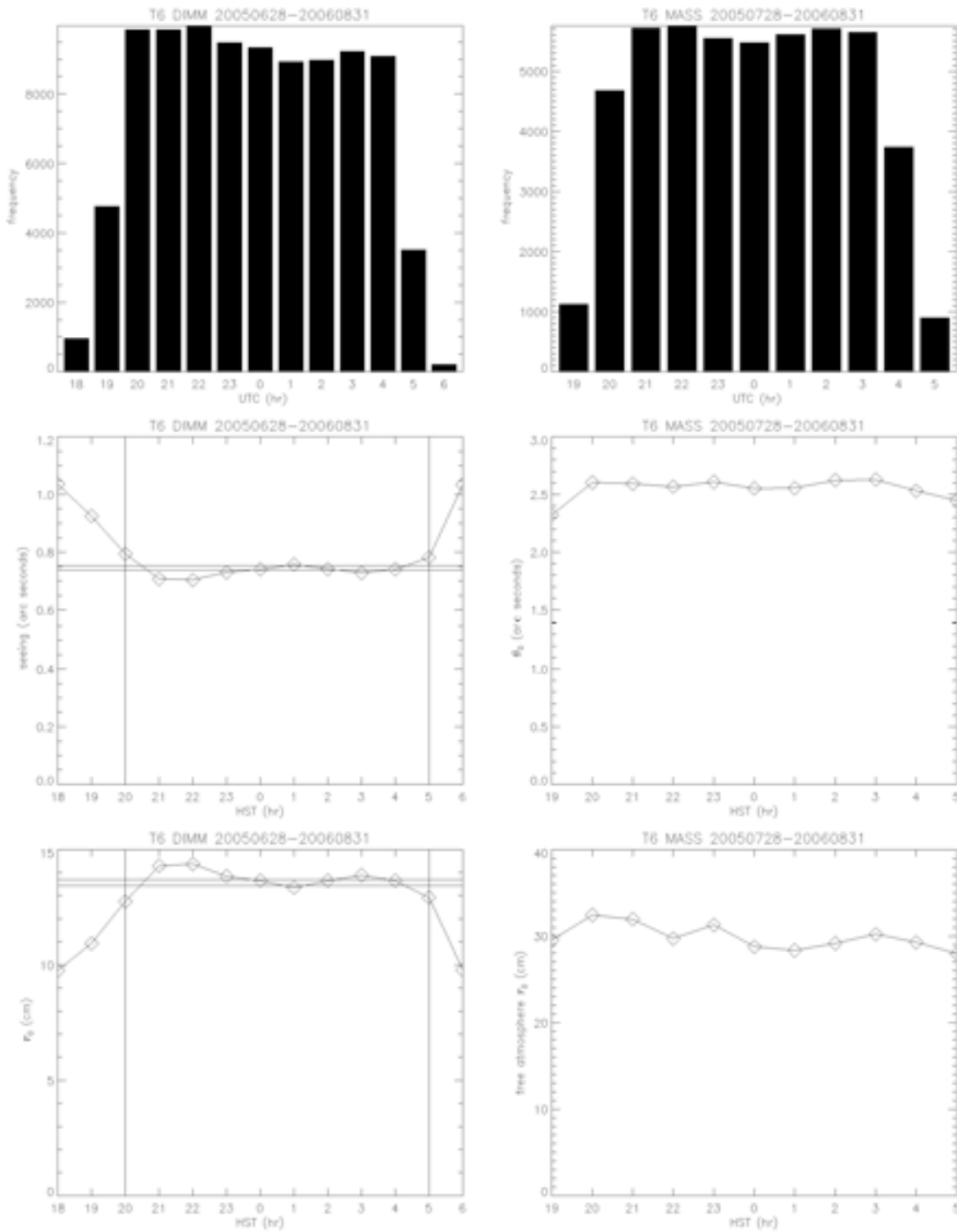


Fig. 7. Hourly statistics of DIMM (left column) and MASS (right column) operations, referenced to the HST time zone (UTC-10). Top row shows the cumulative frequency of operation. For the seeing (right-middle) and r_0 (right-bottom) plots, the two horizontal lines indicate the total median value computed with (dashed) and without (solid) potential twilight hours included, as indicated by the two dotted vertical lines. For the MASS parameters this comparison produced almost no difference, and was omitted from the plot.



4. Mathematical formulas describing turbulence statistics

The statistical quantities referred to in the text and in the graphs are defined here in their most common formulation. I have largely followed the definitions and notation of Ref. [4] (Hardy, 1998).

4.1. Turbulence moments

The m^{th} turbulence moment μ_m , and its upper and lower partial moments μ_m^+ and μ_m^- , are defined at zenith as

$$\mu_m = \int_0^\infty dh h^m C_n^2(h) \quad (1)$$

$$\mu_m^+(H) = \int_H^\infty dh h^m C_n^2(h) \quad (2)$$

$$\mu_m^-(H) = \int_0^H dh h^m C_n^2(h) \quad (3)$$

where h is the altitude variable, H is a given fixed altitude, and $C_n^2(h)$ is the refractive index structure constant (as a function of altitude) in units of $m^{-2/3}$. At non-zero zenith angles ζ the turbulence moments must be multiplied by $\sec^{m+1}(\zeta)$, but in order to make the zenith dependence explicit in the formulas of the next section, the term has been pulled out of the definition here. The m^{th} wind moment w_m is similarly defined as

$$w_m = \int_0^\infty dh v^m(h) C_n^2(h) \quad (4)$$

where $v(h)$ is the wind speed as a function of altitude.

4.2. Statistical quantities

The temporal structure function D_φ of a stochastic variable φ is defined as

$$D_\varphi(\tau) = \langle \|\varphi(t) - \varphi(t + \tau)\|^2 \rangle \quad (5)$$

Using the statistical moments given above, the quantities most commonly used for describing turbulence statistics under Kolmogorov theory can be compactly formulated as

Fried parameter:
$$r_0^{-5/3} = 0.423k^2 \sec(\zeta) \mu_0 \quad (6)$$

Isoplanatic angle:
$$\theta_0^{-5/3} = 2.914k^2 \sec^{8/3}(\zeta) \mu_{5/3} \quad (7)$$

Greenwood frequency:
$$f_G^{5/3} = 0.102k^2 \sec(\zeta) w^{5/3} \quad (8)$$

FA (at zenith):
$$d_0^{-5/3}(H) = k^2 \left[0.5 \mu_{5/3}^-(H) H^{-5/3} - 0.452 \mu_2^-(H) H^{-2} \right] \quad (9)$$



The wavelength dependence enters through the wave number $k=2\pi/\lambda$, and the LGS focal anisoplanatism (FA) parameter d_0 in Eqn. (9) has been simplified from its original expression under the assumption that μ_0^+ is negligibly small for sodium beacons at $H \approx 90$ km. Other useful expressions include the seeing- r_0 relationship

$$\theta = 0.98 \frac{\lambda}{r_0} \quad (10)$$

and inverting Eqn. (6) yields the 0th order turbulence moment in terms of the Fried parameter:

$$\mu_0 = 0.06\lambda^2 r_0^{-5/3} \quad (11)$$

It is common in modeling and analysis to use a discrete model of the atmosphere with a given number N_L of thin layers, by expressing the refractive index structure constant as

$$C_n^2(h) = \sum_{l=1}^{N_L} c_l \delta(h - h_l) \quad (12)$$

where δ is Dirac's delta function. The c_l coefficients represent the contribution to the integrated seeing from individual layers (in a convenient algebraic representation rather than physical) as obtained by integrating $C_n^2(h)$ over a finite range:

$$c_l = \int_0^\infty dh g_l(h) C_n^2(h) \quad (13)$$

where $g_l(h)$ is an appropriate weighting function that asymptotes to zero (e.g. a linear spline, Gaussian, Hanning window, etc) and is centered on the altitude h_l . This is the intrinsic format on which the MASS unit does its estimation of $C_n^2(h)$, whereby it returns the coefficients c_l of a 6-layer profile starting from $h = 500$ meters. The MASS does not measure the ground layer, c_0 , which must be obtained from a combination of DIMM and MASS data. In this study we computed the ground layer simply as

$$c_0 = \mu_0 - \sum_{l=1}^{N_L} c_l \quad (14)$$

where μ_0 was computed from the DIMM seeing according to Eqns. (10) and (11). The isoplanatic angle is also easily computed from the MASS data by substituting (12) into (7), which gives

$$\theta_0 = \left[2.914k^2 \sum_{l=1}^{N_L} c_l h_l^{5/3} \right]^{-3/5} \quad (15)$$

and an estimate of the free atmosphere seeing θ^* can be computed similarly as

$$\theta^* \approx \lambda \left[0.423k^2 \sum_{l=1}^{N_L} c_l \right]^{3/5} \quad (16)$$